Correlation of fatty acids, glyceride core aldehydes, and polycyclic aromatic hydrocarbons during the thermal oxidation of hazelnut oil

Zixuan Liu, Meichu Liu, Zhaoxia Wu, Chunmao Lyu*, Xinyao Jiao, Hongyu Jiang

College of Food Science, Shenyang Agricultural University, Shenyang, China

***Corresponding Author:** Chunmao Lyu, College of Food Science, Shenyang Agricultural University. Email: syaulcm70@syau.edu.cn

Received: 21 December 2023; Accepted: 17 July 2024; Published: 7 August 2024

RESEARCH ARTICLE

Abstract

Fatty acids in edible oil will be oxidized into aldehydes and ketones during hot processing, which will produce polycyclic aromatic hydrocarbons (PAHs) and other harmful substances to human health. Hazelnut oil was heated under different temperatures and times. For each type of oil sample, fatty acid composition, glyceride core aldehyde (GCAs), and PAHs were investigated. The correlation between these indicators was analyzed by the Pearson correlation coefficient. As the main component of hazelnut oil, oleic acid plays an essential role in the formation of GCAs. For GCAs, 9-oxo and 10-oxo-8 compounds were detected. The content of 9-oxo increased with the temperature, while there was no significant change in 10-oxo-8. There exist 15 kinds of PAHs in hazelnut oil. Correlation result shows that GCAs were strongly correlated with six kinds of PAHs (BaA, CHR, BbF, PYR, BaP, and IPY), which shows that GCAs are the precursor of several kinds of PAHs. The research provides strong theoretical guidance for the edible safety and control methods of hazelnut oil.

Keywords: correlation; edible safety; fatty acids; glyceride core aldehydes; polycyclic aromatic hydrocarbons

Introduction

Hazelnut oil, recognized as a premium edible oil, is characterized by its high unsaturated fatty acid content. However, when exposed to oxygen in the air, these unsaturated fatty acids can undergo oxidation. This reaction can result in the formation of short-chain carbon compounds such as ketones, aldehydes, and certain acidic substances. Additionally, the oxidation process can impart a pungent and distinctive odor to the oil. Over time, these chemical changes can lead to a significant reduction in the oil's quality, and in some cases, may even render it unfit for consumption (Picklo *et al.*, 2011). During high temperatures, this process will be strengthened, and more complex chemical reactions will occur. Therefore, thermal oxidation is worth an in-depth study, especially for hazelnut oil. During thermal oxidation, including processes such as hydrolysis and thermal polymerization (Nachay, 2011), various compounds will form. These include hydroxyl fatty acids, TAG oxide monomers, polymerization products, trans-fatty acids, sterol derivatives, and other substances (Guillen and Uriarte, 2012).

Glyceride core aldehydes (GCAs) are a class of non-volatile higher aldehydes formed during lipid oxidation, which are often bonded to other scaffolds (sterols, triglycerides, and phosphoesters) by acyl groups. Aldehydes have long been focused on due to their genotoxic and cytotoxic molecules, whose toxic mechanisms involve the formation of adjuncts with biomacromolecules (DNA and proteins) that lead to cell inactivation. Non-volatile aldehydes have lipophilic properties, which can directly act on biofilm after ingestion by the human body through edible oil, leading to the destruction of biofilm structure (Edenharder *et al.*, 1998). α,β oxidized unsaturated aldehydes, which are active in nature, are a type of free

ISSN 1757-837X online, DOI 10.15586/qas.v16i3.1441

aldehydes produced by the degradation of hydroperoxides of unsaturated fatty acids (Zarkovic, 2003). Additionally, 4-hydroxy-2-trans-nonenal (HNE) is suspected to be associated with liver disease, atherosclerosis, Alzheimer's disease, Parkinson's disease, and Huntington's syndrome (Csallany *et al*., 2015). It can also cause DNA and mitochondrial damage, affecting the expression of cancer-related proteins (Pryor and Porter, 1990).

It is well-known that polycyclic aromatic hydrocarbons (PAHs) are one of the IARC Type 1 carcinogens. PAHs are mainly ingested by the human body through food (Sartori and Gaion, 2016). During the frying process, the elevated temperatures within the system facilitate extensive substance interchange and chemical reactions. Consequently, harmful substances can be inadvertently ingested by individuals through the consumption of fats (Dragana *et al.*, 2023). So the safety of edible oil has been widely concerned (Purcaro *et al.*, 2013). Thus, the quality of frying oils should be controlled.

Over the past few years, there has been a notable increase in the application of statistical methods, machine learning techniques, and computer vision within the field of food analysis (Abamba *et al*., 2021; Fan *et al*., 2020). Techniques such as principal component analysis (PCA) have become particularly prevalent in the analysis of food imagery (Rodríguez *et al*., 2018). Additionally, cross-correlation, a more recent addition to the analytical toolkit, has been employed to study the structure and distribution of gels and fats in microscopic images of various food systems (Glover *et al*., 2019; Gregersen *et al.*, 2021). Furthermore, conducting correlation analysis on the production of oil oxidation can shed light on the pathways leading to the formation of harmful substances.

Previous studies have indicated a strong correlation between the formation of PAHs and the content of polar components in the hot processing of edible oil (Zhu *et al*., 2018). Due to the polarity of GCAs, the generation of PAHs is probably related to GCAs. In the current research, a correlation model was developed using Pearson's method to explore the link between the formation of GCAs and PAHs. Under conditions of thermal oxidation, which are quite complex, the study deduced the formation pathway of PAHs, known to be potent carcinogens, by correlating them with the harmful byproducts resulting from the autooxidation of oil.

Materials and Methods

Materials and reagents

Hazelnut oil, made by cold pressing (purchased from Tieling Sanneng Hazelnut Oil Co., LTD). n-hexane, KOH, HCl, methyl tert-butyl ether, sulfuric acid-methanol, Methyl pentadecanoate, sodium sulfate, acetone, isooctane, and methylene chloride were purchased from Sinopharm Chemical Reagent Group Co., Ltd. (SCRC), Shanghai, China.

Oil sample hot processing

Hazelnut oil underwent heating treatments at temperatures of 60°C, 90°C, 120°C, 150°C, 180°C, and 210°C for both 5 and 10 min. This range encompasses temperatures commonly used in everyday life and in various production processes, including cold blending, mild heat treatment, slight warming, and deep frying. The study encompassed a total of 14 distinct treatments, with each treatment being replicated three times.

For the procedure, 50 mL of hazelnut oil were poured into a 250 mL beaker. The beaker was then placed in an electric water bath with a thermostatic control (model XMTD-8222, manufactured by Guohua Electric Appliance Co., LTD) for heating to the designated temperature and time. After processing, the samples were stored at a temperature of -20°C.

Fatty acid composition

Fatty acids were methylated and chemically converted into their volatile esters in transesterification reaction. Fatty acid methyl esters (FAME) were prepared according to the method by Kravic *et al*. (2010) with some modifications. 170 μL of hazelnut oil and 2.4 mL of n-hexane were added to a test tube with a stopper. Then, 0.6 mL of 2 mol/L KOH in methanol was added and shaken for 20 s. Following this, the closed test tube was placed in a heated water bath at 70°C for 1 min, after which it was removed from the water bath and shaken for 20 s. Afterwards, 1.2 mL of 1 mol/L HCl in methanol was added to the tube and left until separated into two phases. After phase separation, 1 μL of fatty methyl esters in n-hexane (upper phase) was injected into the gas chromatograph (Dragana *et al*., 2023), with three replicates per treatment.

The gas chromatography-mass spectrometry (GC-MS) analysis was conducted using an Agilent 7890-5975 instrument (Agilent Technologies, America International Pte. Ltd). An HP-FFAP (30 m×0.250 mm×0.25 μm) elastic quartz capillary column was used for gas chromatography. The heating procedure consisted of an initial temperature of 50°C, then rising to 250°C at 10°C/min for 5 min, the vaporization temperature was 260°C. The carrier gas was helium at a 0.4 MPa pressure and an injection volume of 1 μL. The area normalization method was used for quantitative analysis. The relative content

of each component were obtained, and the total unsaturated fatty acids, monounsaturated fatty acids, and polyunsaturated fatty acids were calculated.

Determination of GCAs

The GCA was determined using the method described in one of our previous research studies (Liu *et al*., 2022).

A 300 mg sample was accurately weighed into a 50 mL capped centrifuge tube. To this, 100 µL of an internal standard solution at a concentration of 1 mg/mL, 3 mL of tert-butylmethyl ether, and 2 mL of a 0.2 M sodium methoxide solution were sequentially added. The tube was securely sealed and mixed for 1 min on a vortex oscillator (model UVS-1, Beijing Yousheng United Technology Co., LTD), followed by a 2-min equilibration period at room temperature (25°C). Subsequently, 0.1 mL of a 0.5 M sulfuric acid-methanol solution was introduced to neutralize the generated base, followed by a 5-second vortex mixing. Afterward, 3 mL of ultrapure water was added, and the mixture was vortexed for 10 s at a speed of 3500 revolutions per minute (r/min), then centrifuged for 5 min. The supernatant organic layer was carefully transferred to a 5 mL pressure-capped centrifuge tube, and a nitrogen blower at 45°C was used to evaporate the solvent. Once the solvent had fully evaporated, the residue was reconstituted in 1 mL of HPLC-grade n-hexane, to which anhydrous sodium sulfate was added and vortex mixed for 2 s. The sample solution was then drawn up using a 1 mL disposable syringe, filtered through a 0.22 µm organic filter membrane, and transferred into a 2 mL brown sample vial. This process being repeated three times for each sample to ensure reproducibility. The gas GC-MS analysis was performed using an Agilent 7890-5975 instrument (Agilent Technologies, America International Pte. Ltd). An HP-INNOWAX (30 m × 0.250 mm × 0.25 µm) polydimethylsiloxane-coated fused silica capillary column was utilized for the gas chromatography separation.

GC conditions: The heating procedure is as follows: the initial temperature was 90°C for 2 min, then the temperature was raised to 240°C at 6°C/min, and maintained at 240°C for 10 min. The temperature of the detector and injector was 250°C. The injection volume was 1.0 µL with a split ratio of 1:40 For split injection using high purity He as the carrier gas at a flow rate of 1.2 mL/min. The MS conditions were: 250°C transmission line temperature, 200°C ion source temperature, electron spray ionization (ESI) ionization mode, and 70 eV electron bombardment energy. The scanning range is 40–240 with scanning speed of 0.2 scan/s in full scan mode. The chromatographic peaks of each target component were automatically integrated, and their contents were calculated by the internal standard method. The quantitative formula is as follows:

$$m_i = \frac{A_i}{A_{is}} \times f_i' \times \alpha$$

where, m_i is the GCAs content (mg), A_i is the methyl aldehyde esters (core methyl aldehyde esters peak area), A_{is} is the peak area of the internal reference material, m_i is the mass of the internal standard added to the sample (0.1 mg), f_i is the relative correction factor of 1, α is the conversion factor of methyl aldehyde ester into GCAs content, α(9-oxo) = 4.16 and α(10-oxo-8) = 3.96.

Determination of PAHs

Standard solution configuration

A stock solution containing a blend of 16 priority PAHs was procured from Merck in Sao Paulo, SP, Brazil, with a 10 mg/L concentration. This mixture encompasses a range of PAHs including Naphthalene (NAP), Acenaphthylene (ANY), Acenaphthene (ANA), Fluorene (FLU), Phenanthrene (PHE), Anthracene (ANT), Fluoranthene (FLT), Pyrene (PYR), Benzo[a]anthracene (BaA), Chrysene (CHR), Benzo[b]fluoranthene (BbF), Benzo[k]fluoranthene (BkF), benzo[a]pyrene (BaP), Indeno[1,2,3-cd]pyrene (IPY), Dibenzo[a,h]anthracene (DBA), and Benzo[g,h,i]perylene (BPE). For the development of a calibration curve, several standard solutions were prepared at different concentrations:

- An initial standard solution was made at a concentration of 100.0 ng/mL, from which aliquots of 20.0 µL, 40.0 µL, 50.0 µL, and 80.0 µL were taken using eight injection bottles.
- A second standard solution was prepared at a higher concentration of 500.0 ng/mL, with aliquots of 20.0 µL, 40.0 µL, 50.0 µL, and 100.0 µL being used.
- A dilute series of standard solutions were also prepared with concentrations varying from 10.0 ng/mL to 250.0 ng/mL. These were made up to a final volume of 200.0 µL using a solvent mixture of acetone and isooctane in a 1:1 ratio.

This methodical preparation of standard solutions allows for the accurate quantification and analysis of PAHs in various samples, ensuring the reliability of the results obtained from subsequent analytical techniques such as GC-MS.

Sample pretreatment

First, precisely weigh out 1.000 g of the oil sample and place it into a 15 mL centrifuge tube. Then, add 5 mL

of a 0.3 M (0.3 mol/L) potassium hydroxide (KOH) ethanol solution to the tube and ensure the contents are thoroughly mixed. Allow the mixture to stand at room temperature for a period of 5 min to facilitate the reaction. After the reaction time has elapsed, introduce 4 mL of distilled water and 5 mL of n-hexane into the tube. Proceed to vortex the mixture for 2 min to achieve a homogeneous extraction. This step aids in the partitioning of the components between the aqueous and organic phases. Following the vortex mixing, centrifuge the tube at a speed of 10,000 revolutions per minute (r/min) for 2 min. This step will help to separate the layers within the mixture more distinctly. Once centrifugation is complete, carefully remove and set aside the upper organic layer, which contains the extracted compounds. This upper layer solution will then be subjected to further purification steps to isolate and concentrate the desired components for analysis or testing.

About 5 g of anhydrous sodium sulfate was added to the chromatography column filled with 30 g neutral alumina, and the column was washed with 10 mL methylene chloride and 10 mL n-hexane successively. All the extract was transferred to the column, and the flow rate was controlled at about 1.0 mL/min. After all the extract passed through the packing layer, 20 mL n-hexane was first used to remove impurities. Then, 20 mL methylene chloride-ethyl acetate (1:1) was eluted, the eluent was collected, concentrated by rotary evaporation at 40°C, transferred to 10 mL cone bottom test tube, dried with nitrogen gas at 40°C, added 0.1 mL acetone-isooctane (1:1) solution vortex to dissolve the residue, and transferred to the sample bottle for GC-MS determination.

GC-MS

The GC-MS analysis was conducted utilizing an Agilent 7890-5975 instrument (Agilent Technologies, America International Pte. Ltd). Agilent DB-EUPAH quartz capillary column (30m*0.25*0.25) was used.

GC condition. The injection port temperature was set to 280°C, with He as the carrier gas. The injection volume was 2 μL without shitter. The initial temperature was 80°C for 2 min, then increased to 250°C at 10°C/min for 2 min. After this, it was increased to 315°C at 80°C for 5 min, and finally increased to 320°C at 20°C/min for 5 min. The flow rate is maintained at 0.7 mL/min.

MS condition. The ionization mode is EI, energy 70 eV, ion source temperature 230°C, transmission line temperature 280°C, quadrupole temperature 150°C, and ion monitoring.

Data collation and analysis

Excel 2016 was used for data collation, Origin2021 Pro was used for graphs, and SPSS 23 was used for one-way ANOVA and Pearson correlation analysis of data. Each group of tests was repeated three times and parallel three times.

Results and Discussion

Changes in fatty acid composition during heat treatment

As shown in Table 1, hazelnut oil is constituted of five fatty acids, which are palmitic acid, palmitoleic acid, stearic acid, oleic acid, and linoleic acid. Among them, palmitic acid and stearic acid are saturated fatty acids. Palmitoleic acid, oleic acid, and linoleic acid are unsaturated fatty acids. During the thermal processing, the oleic acid content was always upward, while the linoleic acid content showed a downward trend. When heated for 5 min, the content of oleic acid increased from 81.08% to 81.88%, and the content of linoleic acid decreased from 7.42% to 7.23%. When heated for 10 min, the content of oleic acid increased to 81.92%, and the content of linoleic acid decreased to 7.10%, increasing oleic acid content, which is similar to the research before (Nana *et al*., 2022). However, the palmitic acid, palmitoleic acid, and stearic acid contents did not change significantly.

The reason for the decrease in linoleic acid content may be that the polyunsaturated structure of linoleic acid was oxidized, and some of it was converted into monounsaturated fatty acid, which existed in the oil system with the same structure of oleic acid. The reason for the almost no change in the content of other types of fatty acids may be that their properties are more stable, and they are not easy to decompose or transform under the heating conditions used in this paper.

This part of the data is based on one of our previous studies (Liu *et al*., 2022). This section is divided into subheadings, which provide a concise and precise description of the experimental results, their interpretation, as well as the experimental conclusions that can be drawn.

Changes in glyceride core aldehyde content

In previous studies, people mainly studied the small molecules with volatile aldehydes produced in the process of thermal oxidation of edible oils. Non-volatile aldehydes are often ignored and directly absorbed by the human body, causing harm to the body. GCAs are one of the common non-volatile aldehydes in edible oil.

As shown in Figure 1A,B, two kinds of GCAs were detected during heat treatment of hazelnut oil, they are 9-oxo and 10-oxo-8. Hazelnut oil, which has not been superheated, contains about 80% 10-oxo-8 and the rest is mostly 9-oxo. The results are consistent with previous research (Wu *et al*., 2022). As shown in Figure 1C,

Table 1. Changes in fatty acid composition during heat treatment.

Fatty acid	Molecular formula	Heating time/min	Content/%						
			20°C	60°C	90°C	120°C	150°C	180°C	210°C
Palmitic acid	C16:0	5	4.93±0.11^{a}	5.15±0.18^{a}	5.04±0.12^{a}	5.10±0.06^{a}	5.06±0.29^{a}	4.99±0.11^{a}	5.31±0.06^{a}
		10	4.93±0.11^{a}	5.15±0.18^{a}	5.10±0.15^{a}	5.14±0.16^{a}	5.17±0.15^{a}	5.02±0.20^{a}	5.21±0.06^{a}
Palmitoleic acid	C16:1	5	0.18±0.06^{a}	0.15±0.10^{a}	0.19±0.08^{a}	0.15±0.08^{a}	0.19±0.06^{a}	0.16±0.06^{a}	0.17±0.08^{a}
		10	0.18±0.06^{a}	0.16±0.04^{a}	0.18±0.08^{a}	0.17±0.08^{a}	0.17±0.08^{a}	0.16±0.07^{a}	0.15±0.08^{a}
Stearic acid	C18:0	5	1.96±0.10^{a}	1.86±0.08^{a}	1.99±0.09^{a}	1.93±0.08^{a}	1.89±0.11^{a}	1.94±0.07^{a}	1.99±0.06^{a}
		10	1.96±0.10^{a}	1.90±0.06^{a}	1.98±0.10^{a}	1.95±0.02^{a}	1.86±0.21^{a}	1.96±0.06^{a}	1.97±0.04^{a}
Oleic acid	C18:1	5	81.08±0.06^{d}	81.09±0.09^{d}	81.55±0.06^{cd}	81.61±0.05^{cd}	81.69±0.08^{c}	81.75±0.08^{b}	81.88±0.09^{a}
		10	81.08±0.06^{e}	81.13±0.06d^{e}	81.63±0.06^{de}	81.70±0.09^{d}	81.82±0.10^{c}	81.86±0.06^{b}	81.92±0.05^{a}
Linoleic acid	C18:2	5	7.42±0.02^{a}	7.34±0.01^{b}	7.29±0.02^{c}	7.28±0.02^{c}	7.26±0.02^{d}	7.24±0.03^{de}	7.23±0.02d^{e}
		10	7.42±0.02^{a}	7.33±0.02^{b}	7.26±0.03^{c}	7.20±0.02^{d}	7.16±0.04^{e}	7.13±0.06^{f}	7.10±0.05^{f}

Data are presented as mean±SD (n=10). Mean values with different superscript letters are statistically different (p≤0.05) among the groups.
$^{a\text{-}f}$Values with different superscripts in the same row are significantly different (p≤0.05).

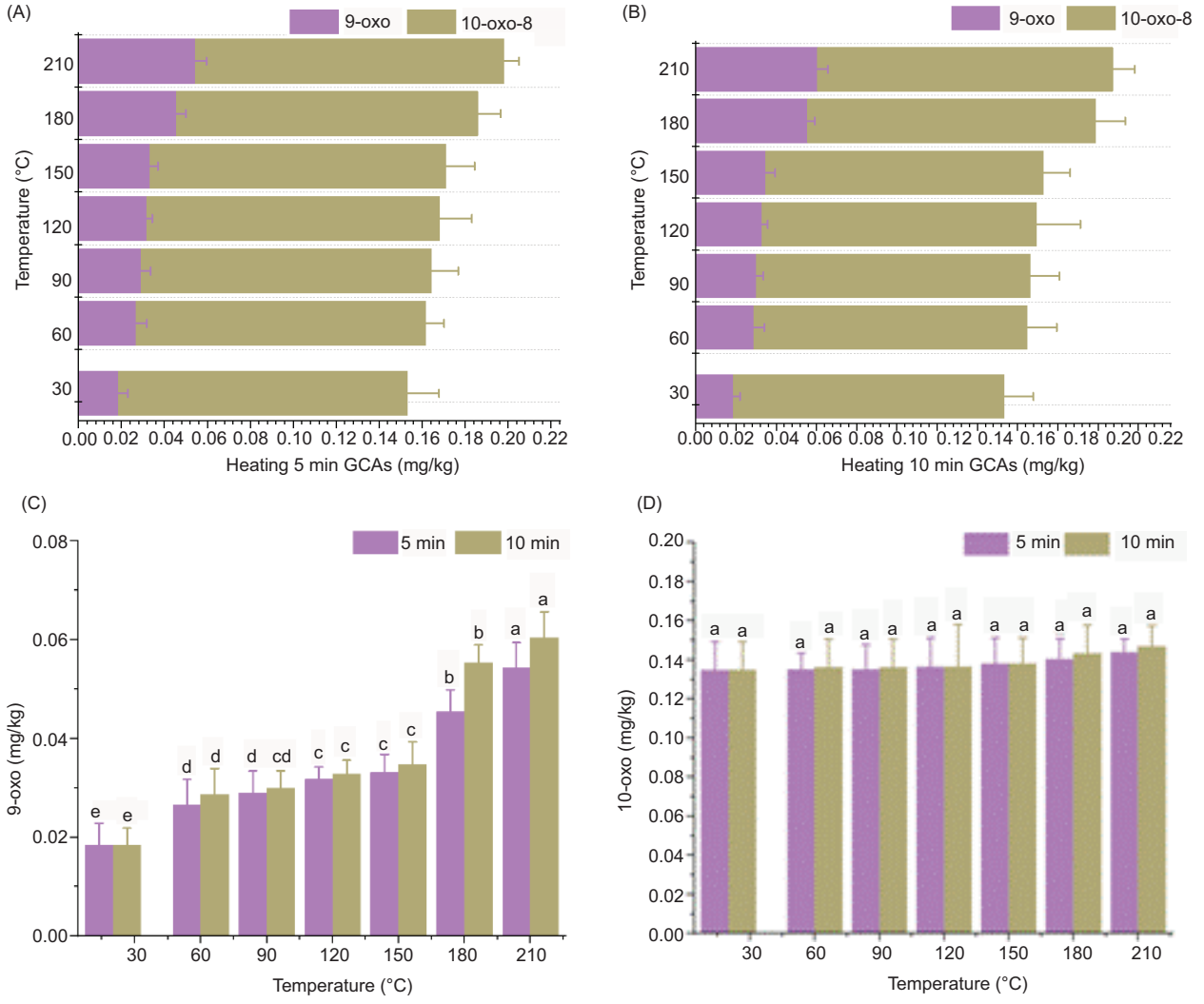

Figure 1. Changes in core aldehyde content. (A) Changes in GCAs during heating for 5 min. (B) Changes in GCAs during heating for 10 min. (C) Changes in the content of 9-oxo during heat treatment. (D) Changes in the content of 10-oxo-8 during heat treatment.

the content of 9-oxo increased significantly with the increase in heat treatment temperature, while the content of 10-oxo-8 did not change significantly with the increase in heat treatment temperature (Figure 1D). This is because the formation rate of 10-oxo-8 is low or the conversion rate is fast in the process of oil thermal oxidation. When the heating temperature is higher than 150°C, the 9-oxo production rate increases significantly, indicating that hazelnut oil may not be suitable for hot processing above 150°C. Therefore, the main GCAs generated in the heat treatment process are 9-oxo, and 10-oxo-8 is likely to be generated only at room temperature.

The thermal oxidation of vegetable oils proceeds through a distinct set of reactions when compared to autooxidation and enzymatic oxidation at ambient temperatures. Consequently, specific compounds like 9-oxo are predominantly formed during the thermal oxidation process of oils. In contrast, at room temperature, autooxidation, photooxidation, and enzymatic oxidation are more likely to lead to the formation of 10-oxo-8. As highlighted by (Chen and Chiou (1995), the presence of lipoxygenase (LOX) can significantly enhance the rate of oil oxidation at room temperature. In the current study, cold-pressed hazelnut oil was utilized, a method that preserves the activity of lipoxygenase throughout the oil production process. As such, enzymatic oxidation could also contribute to the generation of 10-oxo-8.

The hazelnut oil selected for this study contains over 80% oleic acid. The correlation analysis conducted revealed a significant Pearson correlation coefficient between the content of oleic acid and the content of GCAs at a p-value of 0.01, indicating a strong relationship. This statistical significance suggests that oleic acid can be identified as a precursor in the formation of GCAs, which are compounds of interest in the study of oil oxidation and quality.

PAHs standard curve

The standard curve was developed by plotting the ratio of the concentration of each targeted PAH to the concentration of its respective internal standard (IS) on the x-axis. Using these coordinates, a linear regression equation and the correlation coefficient were calculated for each PAH to establish the standard curve (Table 2).

Out of the 16 PAHs analyzed, all except for IPY and DBA demonstrated a strong linear relationship, as evidenced by correlation coefficients exceeding the threshold of 0.999. This high degree of linearity indicates a reliable standard curve for the quantification of PAHs.

PAHs content in crude oil

The content of PAHs in hazelnut oil that has not undergone overheating treatment was assessed and the findings are presented in Table 3. The presence of PAHs in crude hazelnut oil can be attributed to environmental contamination during the growth of the raw material, potentially through exposure to polluted wastewater and waste gases, which facilitates the transfer of PAHs to the oil seeds. The concentrations of certain PAHs with fewer aromatic rings, such as NAP, FLU, PHE, ANT, FLT, and PYR, were found to exceed 2 micrograms per kilogram (μg/kg) in the hazelnut oil sample. Specifically, the level of BaP was measured at 0.39 μg/kg, which is below the 2 μg/kg threshold stipulated by regulation No. 2021/2317. Except for ANA, which was recorded at 1.24 μg/kg, the levels of other PAHs were below 1 μg/kg. Among the PAHs detected in the crude hazelnut oil, PYR had the highest concentration at 4.09 μg/kg.

Table 2. Standard curve of PAHs.

Target object	Linear equation	r	Content (μg/kg)
NAP	Y = -13906.5+23224.7X	0.9992	2.71±0.04
ANY	Y = -19410.1+30507.3X	0.9997	0.63±0.01
ANA	Y = -6144.79+8972.94X	0.9999	1.24±0.15
FLU	Y = -12196.2+10874.3X	0.9991	2.53±0.23
PHE	Y = -13325.8+16876.8X	0.9994	2.28±0.04
ANT	Y = -11439.5+15274.8X	0.9993	3.26±0.01
FLT	Y = -489.084+18900.7X	0.9999	3.43±0.08
PYR	Y = 31570.6+19661.3X	0.9993	4.09±0.02
BaA	Y = -13906.5+23224.7X	0.9999	0.10±0.01
CHR	Y = -20037.6+21625.5X	0.9999	1.00±0.01
BbF	Y = -928.049+54504X	0.9992	1.08±0.01
BkF	Y = -15129.5+53493.6X	0.9993	-
BaP	Y = -9221.61+51379.7X	0.9990	0.39±0.01
IPY	Y = 115482+79047.2X	0.9986	0.32±0.01
DBA	Y = -24944.9+64698.2X	0.9988	0.36±0.01
BPE	Y = 17055.6+67374.6X	0.9998	0.54±0.04

Table 3. PAHs content in crude oil.

PAHs	Content (μg/kg)	PAHs	Content (μg/kg)
NAP	2.71±0.04	BaA	0.10±0.01
ANY	0.63±0.01	CHR	1.00±0.01
ANA	1.24±0.15	BbF	1.08±0.01
FLU	2.53±0.23	BkF	-
PHE	2.28±0.04	BaP	0.39±0.01
ANT	3.26±0.01	IPY	0.32±0.01
FLT	3.43±0.08	DBA	0.36±0.01
PYR	4.09±0.02	BPE	0.54±0.04
PAH4	2.57	LPAHs	22.35
HPAHs	1.61	PAH16	23.96

In contrast, the concentration of BaA was the lowest at 0.1 μg/kg. Notably, no BkF was detected among the 16 types of PAHs analyzed. The combined concentration of the four priority PAHs (PAH4, which includes BaA, CHR, BbF, and BaP) was 2.57 μg/kg, which is significantly below the regulatory limit of 10 μg/kg as required by No. 1881/2006.

Change of PAHs content during heat treatment

Statistics of polycyclic aromatic hydrocarbons

Figure 2A illustrates the variation in PAH content throughout the entire heat treatment procedure. PAHs are categorized into five groups based on the number of benzene rings they contain, with each group's content variation being individually tallied. The complexity of PAH formation increases with the number of rings, which results in a higher proportion of PAHs with fewer rings within the oil (Drabova *et al.*, 2013). During the heat treatment of vegetable oils, as depicted in Figure 2, the concentration of PAHs with 2–4 benzene rings is notably higher compared to those with 5–6 rings. This trend can be attributed to the fact that PAHs with a greater number of rings are more stable and, consequently, more challenging to form. As a result, the proportion of PAHs with fewer rings is disproportionately larger within the oil matrix.

Naphthalene (NAP), the predominant two-ring PAH, exhibits significant fluctuations during the heating process. This is primarily due to its inherent instability, which facilitates both its formation and its subsequent transformation into other PAHs compounds. As for three-ring PAHs, they encompass ANA, ANY, FLU, PHE, and ANT. These compounds are not only the most prevalent PAHs

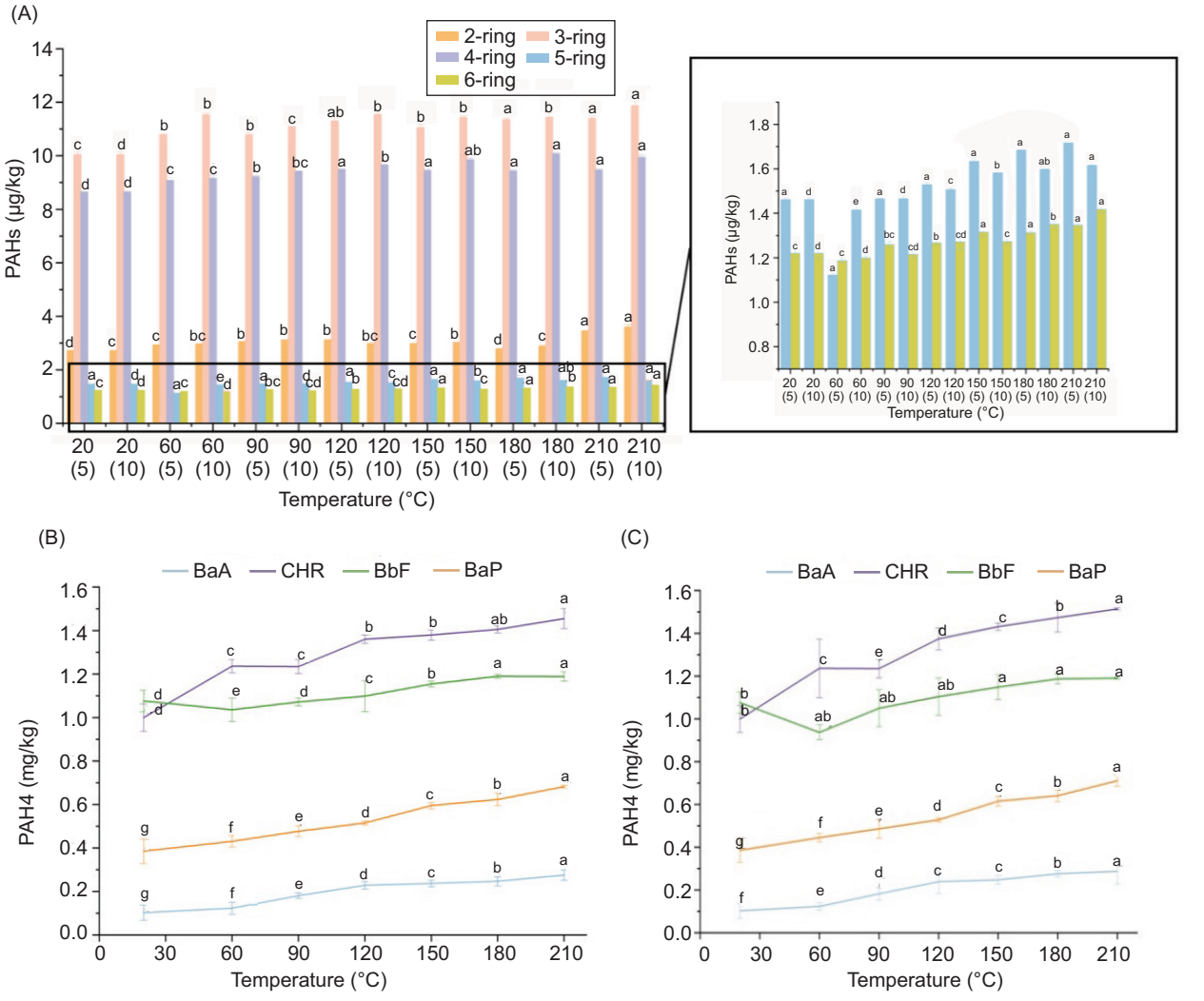

Figure 2. Changes in PAHs content during heat treatment. (A) Change of PAHs content in the whole heat treatment process. (B) PAH4 content during heating for 5 min. (C) PAH4 content during heating for 10 min.

in hazelnut oil but also have a high propensity to undergo chemical reactions that result in the formation of PAHs with a greater number of rings (Farhadian *et al*., 2010). Four-ring PAHs consist of FLT, PYR, BaA, and CHR. The overall content variation of these PAHs during the heat treatment process is not pronounced. This could be due to the absence of precursor substances and the necessary conditions for their formation in hazelnut oil, or it might be because they are more likely to be converted into other compounds. About five-ring PAHs, which include BbF, BkF, BaP, and DBA, these compounds are relatively stable and less prone to transformation. However, under specific conditions, they can undergo further polymerization. Lastly, the six-ring PAHs are primarily represented by IPY and BPE. These types of PAHs are highly stable and, once formed, are not easily transformed or decomposed. As a result, there is a slight increase in the content of six-ring PAHs.

Change of PAH4 content

The European Food Safety Authority (EFSA) has identified PAH4 as a benchmark index for assessing PAHs in the food industry. The PAH4 index encompasses four specific PAHs: BaA, CHR, BbF, and BaP. The variations in the levels of these compounds are depicted in Figure 2B,C. According to EFSA guidelines, the permissible maximum concentration of PAH4 in edible oils is set at 10 μg/kg, while for BaP, it is even more stringent at 2 μg/kg. The experimental findings indicate that the combined concentrations of PAH4 and BaP detected did not surpass the safety thresholds established by the EFSA. There is also a part of BaP in lampblack (Ledesma *et al.*, 2015), so the actual amount of BaP produced should exceed the measured value. Prolonged exposure to high temperatures during the oil treatment process poses certain health risks. It is observed, except BbF, the levels of the other PAH4 constituents continue to rise. In contrast, BbF exhibits a slight decline at a temperature of 60°C, which could be attributed to its tendency to volatilize and subsequently be carried away with the exhaust gases post-heating (Mengke *et al*., 2021). Initially, CHR is present in lower concentrations than BbF. However, following the heat treatment process, the levels of CHR surpass those of BbF. This observation suggests that CHR is more thermally reactive than BbF, with a more rapid rate of formation upon exposure to heat.

Correlation analysis

A Pearson correlation analysis was performed to examine the relationship between the levels of unsaturated fatty acids, glycidyl esters of fatty acids (GCAs), and polycyclic aromatic hydrocarbons (PAHs). The findings are visually represented in a heat map (Figure 3A). The analysis revealed that oleic acid has a significant correlation with the formation of both GCAs and various PAHs. Notably, the PAH4 group, which includes BaA, CHR, BbF, and BaP, shows a stronger correlation with the content of GCAs. This suggests a link between the formation of PAH4 and GCAs. Furthermore, the overall formation of PAHs is significantly correlated with the levels of GCAs. Among the PAHs, 9-oxo, which exhibits pronounced changes during the heating process, significantly correlates with the formation of several PAHs, including BaP, CHR, BaA, PYR, and IPY. Understanding the formation mechanism of 9-oxo, which can be inferred from its molecular structure, may provide valuable insights for guiding future research in this area.

Inference of PAHs generation mechanism during heat treatment of hazelnut oil

As shown in Figure 3B, at low temperatures (≤60°C), hydroperoxide is produced by oil under the catalytic oxidation of excessive ions, light and lipoxygenase (LOX). The alkoxy free radical fragment generated by the breakage of -C-C- at the black arrow breaks away from the glycerol skeleton (Ceci and Carelli, 2010). In the subsequent oxidative cracking, free aliphatic aldehydes with different carbon chain lengths (mainly volatile small molecule aldehydes) are formed. The red arrow indicates that the hydroperoxide is decomposed by β-shear to form the secondary oxide 10-oxo-8. Under high-temperature heating conditions (>60°C), LOX is inactivated, and the oil is mainly oxidized by heat (Lledias and Hansberg, 2000). 9-oxo, another secondary oxidation product, is produced. At the later stage of heating, 9-oxo will undergo thermal polymerization through the -C-C- connection to produce oxygen-free ring polymerization products BaA and CHR. The polymerization of 10-oxo-8 will generate pentacyclic aromatic hydrocarbons BaP, and then react with substances with double bonds to produce high ring number PAHs such as IPY and BPE.

Other types of PAHs are generated by the polymerization of free aliphatic aldehydes (Zhangi *et al*., 2019) produced by the oxidative decomposition of alkoxy free radical fragments. Hexal and 2-octen-1-al are the volatile small molecules generated during the oxidation of hazelnut oil, and they can undergo further polymerization reactions. This part mainly generates PAHs with low ring numbers, such as ANY, ANA, PHE, PYR, etc. These PAHs with low ring numbers will further polymerize with NAP to generate PAHs with high ring numbers.

Conclusions

Oleic acid constitutes over 80% of the total fatty acids in hazelnut oil. Correlation analysis has revealed a significant Pearson correlation coefficient between the content of oleic acid and that of GCAs at a p-value of 0.01, indicating a strong relationship. Therefore, oleic acid can be identified as a precursor to the formation

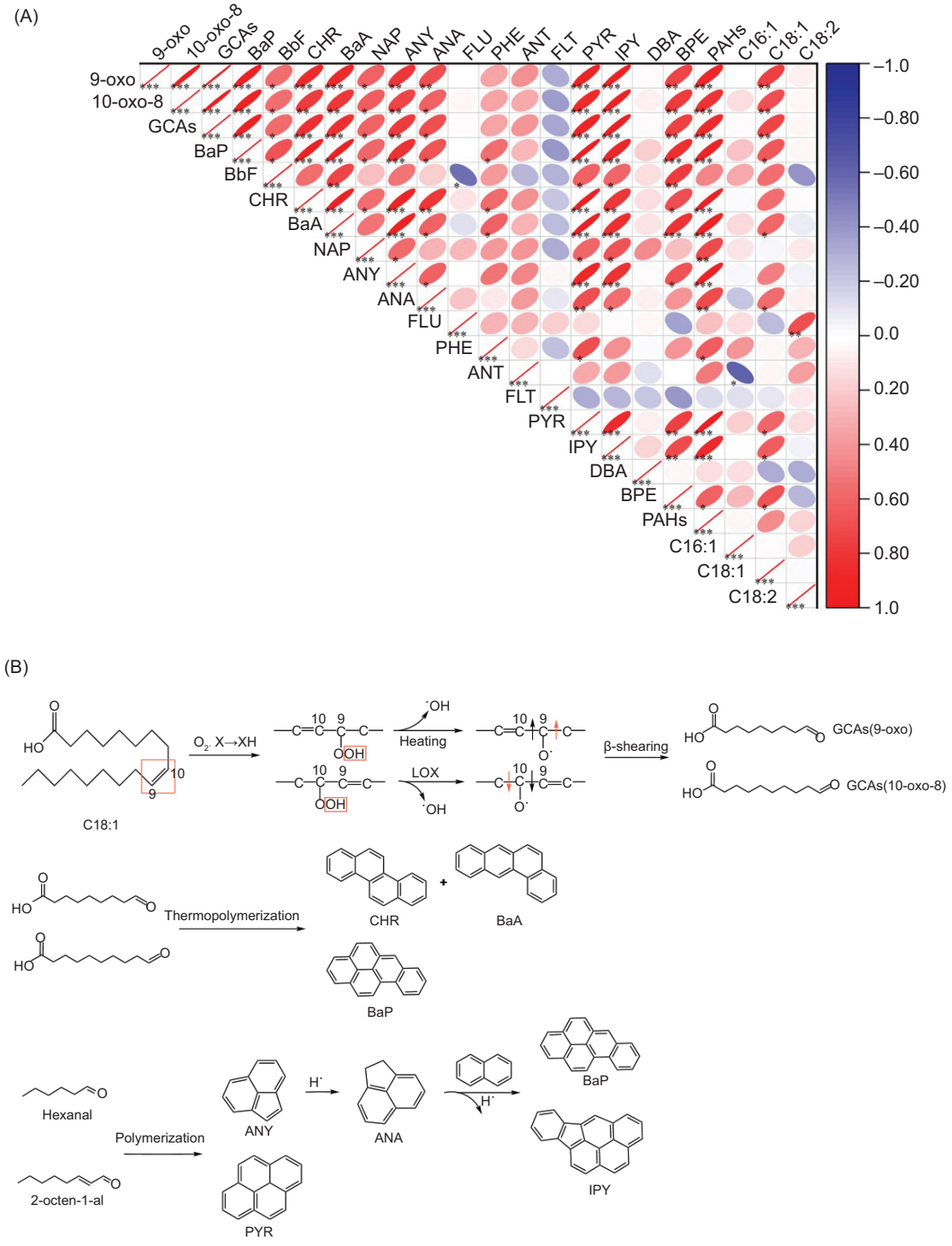

Figure 3. Inference of PAHs generation mechanism. (A) Correlation analysis among each index. (B) Inference of PAHs generation mechanism during heat treatment of hazelnut oil. *p≤0.05 **p≤0.01 ***p≤0.001

of GCAs. Fifteen distinct types of PAHs were detected in hazelnut oil. The analysis of PAHs change under various heat treatment conditions has led to the conclusion that GCAs play a vital role in the formation of a subset of PAHs through thermal polymerization. This includes BaP, which is recognized as one of the most carcinogenic PAHs. The remainder of the PAHs are believed to originate from the thermal polymerization of hexanal and 2-octenal, as well as from reactions involving NAP. This research holds significant implications for the practical use of hazelnut oil in everyday settings, such as storage and cooking. It suggests that hazelnut oil should not be used for frying at temperatures exceeding 150°C due to the potential formation of harmful substances. By identifying the pathways leading to PAH production in oils, this study provides valuable guidance on the risk factors associated with oil oxidation, aiding in the development of strategies to mitigate these risks.

Author Contributions

Conceptualization: Zixuan Liu and Meichu Liu; methodology: Zixuan Liu; software: Xinyao Jiao; validation: Hongyu Jiang and Chunmao Lyu; formal analysis: Xinyao Jiao; investigation: Hongyu Jiang; resources: Zhaoxia Wu; data curation: Meichu Liu; writing—original draft preparation: Zixuan Liu; writing—review and editing: Chunmao Lyu; supervision: Zhaoxia Wu; project administration: Zhaoxia Wu; funding acquisition: Chunmao Lyu. All authors have read and agreed to the published version of the manuscript.

Funding

This research was funded by Key R&D Project of Liaoning Province, under Grant Research and Demonstration of Key Technologies for Deep Processing and Comprehensive Utilization of Northeast Hazelnuts (2020JH2/10200037); Service Local Project of Liaoning Province, under Grant Demonstration and Promotion of new deep-processing technology for comprehensive utilization of Northeast Hazelnuts (LSNFW201903) and horizontal subject, under Grant Demonstration and Promotion of key technologies for transformation and deep processing of wild hazelnut forest in northwestern Liaoning (H2019388).

Data Availability Statement

We encourage all authors of articles published in Codon journals to share their research data. This section provides details regarding where data supporting reported results can be found, including links to publicly archived datasets analyzed or generated during the study. A statement is still required when no new data are created or where data are unavailable due to privacy or ethical restrictions.

Conflicts of Interest

The authors declare no conflicts of interest.

References

Abamba, O. K., Yoshito, S., Huang, Z., Alin, K., Makoto, K., Yuichi, O. et al. 2021. Evaluating Japanese dace (Tribolodon hakonensis) fish freshness during storage using multispectral images from visible and UV excited fluorescence. LWT 151. https://doi.org/10.1016/j.lwt.2021.112207

Ceci, L. N., and Carelli, A. A. 2010. Relation between oxidative stability and composition in argentinian olive oils. Journal of the American Oil Chemists Society 87(10): 1189–1197. https://doi.org/10.1007/s11746-010-1598-6

Chen, M. J., and Chiou, R. Y. 1995. Variation of iron, copper, free fatty acid content and lipoxygenase activity in peanut kernels subjected to various pretreatments and roasting. International Journal of Food Sciences and Nutrition 46(2): 145–148. https://doi.org/10.3109/09637489509012542

Csallany, A. Saari, Han, I., Shoeman, D. W., Chen, C., and Jieyao Y. 2015. 4-Hydroxynonenal (HNE), a toxic aldehyde in french fries from fast food restaurants. Journal of the American Oil Chemists Society 92(10): 1413–1419. https://doi.org/10.1007/s11746-015-2699-z

Drabova, L., Tomaniova, M., Kalachova, K., Kocourek, V., Hajslova, J. and Pulkrabova, J. 2013. Application of solid phase extraction and two-dimensional gas chromatography coupled with time-of-flight mass spectrometry for fast analysis of polycyclic aromatic hydrocarbons in vegetable oils. Food Control 33(2): 489–497. https://doi.org/10.1016/j.foodcont.2013.03.018

Dragana, R., Jelena, M. Jovan, M., Biljana, N., and Dejan, M. 2023. Antibacterial efficiency of adjuvant photodynamic therapy and high-power diode laser in the treatment of young permanent teeth with chronic periapical periodontitis. A prospective clinical study. Photodiagnosis and Photodynamic Therapy 41: 103129. https://doi.org/10.1016/j.pdpdt.2022.103129

Edenharder, R., Kerkhoff, G., and Dunkelberg, H. 1998. Effects of beta-carotene, retinal, riboflavin, alpha-tocopherol and vitamins C and K1 on sister-chromatid exchanges induced by 3-amino-1-methyl-5H-pyrido 4,3-b indole (Trp-P-2) and cyclophosphamide in human lymphocyte cultures. Food and Chemical Toxicology: An International Journal Published for the British Industrial Biological Research Association 36(11): 897–906. https://doi.org/10.1016/s0278-6915(98)00068-4

Fan, S., Li, J., Zhang, Y., Tian, X., Wang, Q., He, X. et al. 2020. On line detection of defective apples using computer vision system combined with deep learning methods. Journal of Food Engineering 286: 110102. https://doi.org/10.1016/j.jfoodeng.2020.110102

Farhadian, A., Jinap, S., Abas, F. and Sakar, Z. I. 2010. Determination of polycyclic aromatic hydrocarbons in grilled meat. Food Control 21(5): 606–610. https://doi.org/10.1016/j.foodcont.2009.09.002

Glover, Z. J., Bisgaard, A.H., Andersen, U., Povey, M.J., Brewer, J. R. and Simonsen, A.C. 2019. Cross-correlation analysis to quantify relative spatial distributions of fat and protein in super-resolution microscopy images of dairy gels. Food Hydrocolloids 97: 105225. https://doi.org/10.1016/j.foodhyd.2019.105225

Gregersen, S. B., Glover, Z.J., Wiking, L., Simonsen, A.C., Bertelsen, K., Pedersen, B. et al. 2021. Microstructure and rheology of acid milk gels and stirred yoghurts – Quantification of process-induced changes by auto- and cross correlation image analysis. Food Hydrocolloids 111. https://doi.org/10.1016/j.foodhyd.2020.106269

Guillen, M. D., and Uriarte, P. S. 2012. Aldehydes contained in edible oils of a very different nature after prolonged heating at frying temperature: Presence of toxic oxygenated α,β unsaturated aldehydes. Food Chemistry 131(3): 915–926. https://doi.org/10.1016/j.foodchem.2011.09.079

Kravic, S., Suturovic, Z. Svarc-Gajic, J., Stojanovic, z. and Pucarevic, M. 2010. Determination of *trans* fatty acids in foodstuffs by gas chromatography-mass spectrometry after simultaneous microwave-assisted extraction-esterification. Journal of the Serbian Chemical Society 75 (6): 803–812. https://doi.org/10.2298/jsc090717051k

Ledesma, E., Rendueles, M. and Diaz, M. 2015. Spanish smoked meat products: Benzo(a)pyrene (BaP) contamination and moisture. Journal of Food Composition and Analysis 37: 87–94. https://doi.org/10.1016/j.jfca.2014.09.004

Liu, Z., Liu, M., Lyu, C., Li, B., Meng, X., Si, X., and Shu, C. 2022. Effect of heat treatment on oxidation of hazelnut oil. Journal of Oleo Science 71(12): 1711–1723. https://doi.org/10.5650/jos.ess22131

Lledias, F., and Hansberg, W. 2000. Catalase modification as a marker for singlet oxygen. Methods in Enzymology 319: 110–119. https://doi.org/10.1016/S0076-6879(00)19013-5

Mengke, S., Qian, J., Jinhu, G., Yuxin, Z., Shuai, C., Ting, Y. et al. 2021. Quality alert from direct discrimination of polycyclic aromatic hydrocarbons in edible oil by liquid-interfacial surface-enhanced Raman spectroscopy. LWT 143. https://doi.org/10.1016/j.lwt.2021.111143

Nachay, K. 2011. Halting lipid oxidation. Food Technology 65(6): 14–15.

Nana, C., Tiantian, Z., Zhentai, H., Zhen, Y., Guixi, W., Qinghua, M. et al. 2022. Characterisation of oil oxidation, fatty acid, carotenoid, squalene and tocopherol components of hazelnut oils obtained from three varieties undergoing oxidation. International Journal of Food Science & Technology 57(6): 3456–3466. https://doi.org/10.1111/ijfs.15669

Picklo, M. J., Azenkeng, A. and Hoffmann, M. R. 2011. *Trans*-4-oxo-2-nonenal potently alters mitochondrial function. Free Radical Biology and Medicine 50(2): 400–407. https://doi.org/10.1016/j.freeradbiomed.2010.11.014

Pryor, W. A., and Porter, N. A. 1990. Suggested mechanisms for the production of 4-hydroxy-2-nonenal from the autoxidation of polyunsaturated fatty acids. Free Radical Biology & Medicine 8(6): 541–543. https://doi.org/10.1016/0891-5849(90)90153-a

Purcaro, G., Moret, S. and Conte, L.S. 2013. Overview on polycyclic aromatic hydrocarbons: Occurrence, legislation and innovative determination in foods. Talanta 105: 292–305. https://doi.org/10.1016/j.talanta.2012.10.041

Rodríguez, F. J., García, A. Pardo, P.J., Chávez, F., and Luque-Baena, R. M. 2018. Study and classification of plum varieties using image analysis and deep learning techniques. Progress in Artificial Intelligence 7(2): 119–127. https://doi.org/10.1007/s13748-017-0137-1

Sartori, D., and Gaion, A. 2016. Toxicity of polyunsaturated aldehydes of diatoms to Indo-Pacific bioindicator organism *Echinometra mathae*i. Drug and Chemical Toxicology 39(2): 124–128. https://doi.org/10.3109/01480545.2015.1041602

Wu, G., Han, S., Zhang, Y., Liu, T.T., Karrar, E., Jin, Q. et al. 2022. Effect of phenolic extracts from *Camellia oleifera* seed cake on the formation of polar compounds, core aldehydes, and monoepoxy oleic acids during deep-fat frying. Food Chemistry 372. https://doi.org/10.1016/j.foodchem.2021.131143

Zarkovic, K. 2003. 4-hydroxynonenal and neurodegenerative diseases. Molecular Aspects of Medicine 24(4–5): 293–303. https://doi.org/10.1016/s0098-2997(03)00024-4

Zhangi, Y., Lyu, C., Meng, X., Dong, W., Guo, H., Su, C. et al. 2019. Effect of storage condition on oil oxidation of flat-European hybrid hazelnut. Journal of Oleo Science 68(10): 939–950. https://doi.org/10.5650/jos.ess19120

Zhu, Y., Li, X., Huang, J., Zhao, C., Qi, J., Jin, Q. et al. 2018. Correlations between polycyclic aromatic hydrocarbons and polar components in edible oils during deep frying of peanuts. Food Control 87: 109–116. https://doi.org/10.1016/j.foodcont.2017.12.011